連星ブラックホール合体と相対論の検証について

Testing GR with Binary Black Hole Mergers

中野寛之（京大理）

Hiroyuki Nakano (Kyoto)

Probing Various Gravitational Theories (Yagi-san)

Consistent with GR?

Numerical Relativity

(Kiuchi-san)

- **Strongest test of GR**
  - Numerical relativity simulation for binary black holes
  - Inspiral-merger-ringdown waveforms

NR waveform

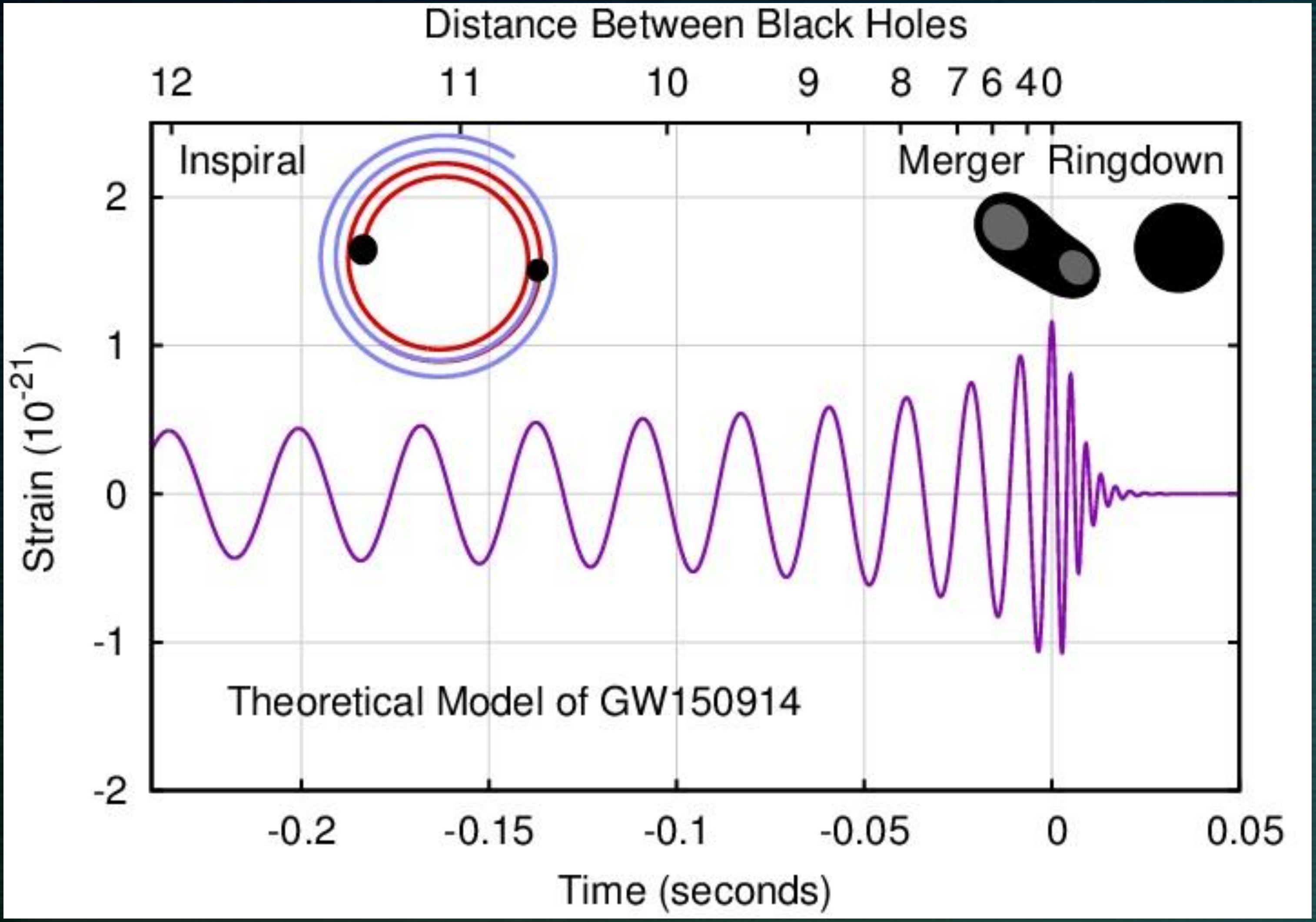

Credits: Carlos O. Lousto and James Healy

Numerical Relativity

(Kiuchi-san)

- **Strongest test of GR**
  - Numerical relativity simulation for binary black holes

- Two papers
  - Directly comparing GW150914 with numerical solutions of Einstein‘s equations for binary black hole coalescence
    Phys. Rev. D 94, 064035 (2016) [arXiv:1606.01262 [gr-qc]].
  - Modeling the source of GW150914 with targeted numerical-relativity simulations
    arXiv:1607.05377 [gr-qc].

Phys. Rev. D 94, 064035 (2016)

- Directly comparing GW150914 with numerical solutions of Einstein's equations for binary black hole coalescence
- 1139 distinct simulations
  - quasicircular inspiral and coalescence
  - 7 parameters (mass ratio (1), spin directions (6))

$$q = m_1/m_2$$

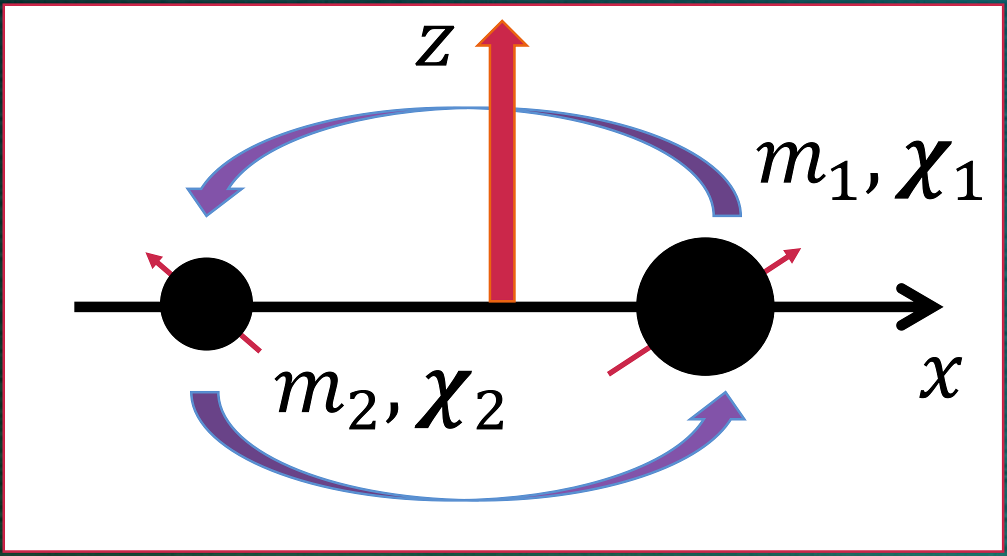

Simulations

Mass ratio / spin / initial orbital frequency / remnant mass / spin

Key	q	$\chi_{1,x}$	$\chi_{1,y}$	$\chi_{1,z}$	$\chi_{2,x}$	$\chi_{2,y}$	$\chi_{2,z}$	$\chi_{\rm eff}$	$M\omega_0$	M_f/M	a_f
D10.50_q0.1667_a0.0_0.0_n100(∗)	6.000	⋯	⋯	⋯	⋯	⋯	⋯	⋯	0.026	0.986	0.372
D10_q0.33_a-0.8_xi0_n100(∗)	2.999	0.757	0.030	0.259	⋯	⋯	−0.800	−0.006	0.029	0.965	0.756
D10_q0.33_a0.8_xi0_n120(∗)	2.999	0.754	0.031	−0.268	⋯	⋯	0.800	−0.001	0.030	0.970	0.607
D10_q0.50_a-0.50_0.50_n100(∗)	2.000	⋯	⋯	0.500	⋯	⋯	−0.500	0.167	0.028	0.953	0.751
D10_q0.50_a-0.8_xi0_n100(∗)	2.000	0.696	0.059	0.392	⋯	−0.006	−0.801	−0.005	0.030	0.956	0.768
SXS:BBH:0001[p]	1.000	⋯	⋯	⋯	⋯	⋯	⋯	⋯	0.012	0.952	0.686
SXS:BBH:0010	1.501	0.248	0.028	−0.433	⋯	⋯	⋯	−0.260	0.014	0.962	0.563
SXS:BBH:0100	1.500	⋯	⋯	⋯	⋯	⋯	⋯	⋯	0.012	0.955	0.664
SXS:BBH:0101	1.501	⋯	⋯	−0.500	⋯	⋯	⋯	−0.300	0.011	0.963	0.540
SXS:BBH:0102	1.500	0.496	0.051	−0.001	0.494	0.071	−0.001	−0.001	0.014	0.954	0.695
RIT:BBH:NQ16TH115PH0	6.000	0.725	⋯	−0.338	⋯	⋯	⋯	−0.290	0.033	0.991	0.554
RIT:BBH:NQ16TH115PH120	6.000	−0.363	0.628	−0.338	⋯	⋯	⋯	−0.290	0.034	0.991	0.552
RIT:BBH:NQ16TH115PH150	6.000	−0.628	0.363	−0.338	⋯	⋯	⋯	−0.290	0.034	0.991	0.556
RIT:BBH:NQ16TH115PH30	6.000	0.628	0.363	−0.338	⋯	⋯	⋯	−0.290	0.032	0.991	0.553
RIT:BBH:NQ16TH115PH60	6.000	0.363	0.628	−0.338	⋯	⋯	⋯	−0.290	0.034	0.991	0.556
RIT:BBH:KTH22.5PH0	1.000	−0.026	0.304	0.760	−0.008	0.310	−0.759	0.001	0.042	0.960	0.695
RIT:BBH:KTH22.5PH120	1.000	−0.272	−0.157	0.757	−0.272	−0.157	−0.757	⋯	0.043	0.961	0.698
RIT:BBH:KTH22.5PH150	1.000	−0.157	−0.272	0.757	−0.157	−0.272	−0.757	⋯	0.043	0.961	0.697
RIT:BBH:KTH22.5PH30	1.000	−0.185	0.257	0.756	−0.157	0.272	−0.757	−0.001	0.042	0.960	0.695
RIT:BBH:KTH22.5PH60	1.000	−0.297	0.138	0.751	−0.272	0.157	−0.757	−0.003	0.042	0.960	0.695
GT:BBH:564	1.000	⋯	⋯	−0.400	⋯	⋯	−0.400	−0.400	0.026	0.961	0.560
GT:BBH:476	1.000	⋯	⋯	−0.200	⋯	⋯	−0.200	−0.200	0.025	0.956	0.624
(0.0,1.0)	1.000	⋯	⋯	⋯	⋯	⋯	⋯	⋯	0.030	0.952	0.686
(0,1.0,'M100')	1.000	⋯	⋯	⋯	⋯	⋯	⋯	⋯	0.029	0.951	0.687
(0.0,1.0,'M120','D11')	1.000	⋯	⋯	⋯	⋯	⋯	⋯	⋯	0.029	0.951	0.686

A simple combination of spins: $\chi_{\rm eff} = (\mathbf{S}_1/m_1 + \mathbf{S}_2/m_2)\cdot \hat{L}/M$,

Phys. Rev. D 94, 064035 (2016)

- Directly comparing GW150914 with numerical solutions of Einstein's equations for binary black hole coalescence
- 1139 distinct simulations
  - quasicircular inspiral and coalescence
  - 7 parameters (mass ratio (1), spin directions (6))
- Redshifted total mass (1)
- 7 extrinsic parameters
  (spacetime coordinates for the event (4),
  Euler angles of binary's orientation (3))
  --> marginalized out

Rankings

Mass ratio / spin / redshifted total mass / start frequency

Key	q	$\chi_{1,x}$	$\chi_{1,y}$	$\chi_{1,z}$	$\chi_{2,x}$	$\chi_{2,y}$	$\chi_{2,z}$	$\chi_{\rm eff}$	$M_z/M_\odot$	$f_{\rm start}$(Hz)
SXS:BBH:0310(∗)	1.221	···	···	···	···	···	···	0.00	73.0	15.1
D12_q1.00_a-0.25_0.25_n100(∗)	1.0	···	···	0.250	···	···	−0.250	−0.00	73.2	20.5
SXS:BBH:0002[S]	1.0	···	···	···	···	···	···	0.00	73.2	10.0
D11_q0.75_a0.0_0.0_n100(∗)	1.333	···	···	···	···	···	···	−0.00	72.1	23.1
SXS:BBH:0305(∗+)	1.221	···	···	0.330	···	···	−0.440	−0.02	74.2	14.8

(**L=2**, m=all), f_{low} = 30Hz

Key	q	$\chi_{1,x}$	$\chi_{1,y}$	$\chi_{1,z}$	$\chi_{2,x}$	$\chi_{2,y}$	$\chi_{2,z}$	$\chi_{\rm eff}$	$M_z/M_\odot$	$f_{\rm start}(Hz)$
SXS:BBH:0002[S]	1.0	···	···	···	···	···	···	0.00	73.2	10.0
SXS:BBH:0307(∗)	1.228	···	···	0.320	···	···	−0.580	−0.08	71.8	16.6
SXS:BBH:0218	1.0	···	···	−0.500	···	···	0.500	0.00	72.8	10.7
D12_q1.00_a-0.25_0.25_n100(∗)	1.0	···	···	0.250	···	···	−0.250	−0.00	73.6	20.4
SXS:BBH:0217	1.0	···	···	−0.600	···	···	0.600	0.00	73.4	11.9
SXS:BBH:0127	1.34	0.010	−0.077	−0.017	−0.061	−0.065	−0.179	−0.09	71.0	14.4
SXS:BBH:0198	1.202	···	···	···	···	···	···	0.00	73.1	12.8
SXS:BBH:0310(∗)	1.221	···	···	···	···	···	···	0.00	72.4	15.2
SXS:BBH:0211	1.0	···	···	−0.900	···	···	0.900	0.00	73.4	11.5
SXS:BBH:0312(∗)	1.203	···	···	0.390	···	···	−0.480	−0.00	73.8	14.8
SXS:BBH:0305(∗+)	1.221	···	···	0.330	···	···	−0.440	−0.02	73.2	15.0

(**L=2 and 3**, m=all), f_{low} = 30Hz

- Uncertainty in parameter estimation

Advertisement

Unless otherwise noted, we extract $\tilde{\psi}_{4,lm}(f)$ [and therefore $\tilde{h}_{lm}(f)$ and $h_{lm}(t)$] at infinity using a perturbative extrapolation [110]

[110] H. Nakano, J. Healy, C. O. Lousto, and Y. Zlochower, Phys. Rev. **D91**, 104022 (2015), arXiv:1503.00718 [gr-qc].

- Gravitational wave at infinity (Weyl scalar ψ_4 from NR)

$$\lim_{r\to\infty} r\psi_4 = \lim_{r\to\infty} r(\ddot{h}_+ - i\ddot{h}_\times).$$

- ψ_4 extracted from a finite radius, need extrapolation

$$r\psi_4^{\ell m}|_{r=\infty} = \left(1 - \frac{2M}{r}\right)\left(r\psi_{4\ell m}^{\rm NR}(t,r) - \frac{(\ell-1)(\ell+2)}{2r}\int dt[r\psi_{4\ell m}^{\rm NR}(t,r)]\right)$$

- But, there is a problem … We will see later.

arXiv:1607.05377 [gr-qc]

- Two completely independent codes

	LazEv RIT	**SpEC** SXS
Initial data		
Formulation of Einstein constraint equations	conformal method using Bowen-York solutions [37–39]	conformal thin sandwich [38, 40]
Singularity treatment	puncture data [41]	quasi-equilibrium black-hole excision [42–44]
Numerical method	pseudo-spectral [45]	pseudo-spectral [46]
Achieving low orbital eccentricity	post-Newtonian inspiral [47]	iterative eccentricity removal [48, 49]
Evolution		
Formulation of Einstein evolution equations	BSSNOK [50–52]	first-order generalized harmonic with constraint damping [11, 53–55]
Gauge conditions	evolved lapse and shift [56–58]	damped harmonic [59]
Singularity treatment	moving punctures [12, 13]	excision [60]
Outer boundary treatment	Sommerfeld	minimally-reflective, constraint-preserving [53, 61]
Discretization	high-order finite-differences [62, 63]	pseudo-spectral methods
Mesh refinement	adaptive mesh refinement [64]	domain decomposition with spectral adaptive mesh refinement [46, 59]

Exception: [38] Pfeiffer and York, Phys. Rev. D 67, 044022 (2003).
A new class of covariant decompositions of the extrinsic curvature

Target

- GW150914

Mass ratio / **spin** / initial frequency / radial velocity / separation / eccentricity

Config.	q	χ_1	χ_2	$M\Omega_0$	$M\dot{a}_0 \times 10^4$	d_0/M	e
RIT	1.220	-0.4400	0.3300	0.02118	-1.1712	12.2500	0.0012
SXS	1.221	-0.4400	0.3300	0.01696	-0.5306	14.2601	0.0008

Difference between waveforms

- Initial parameters for BBH ($M = m_1 + m_2$)

Config.	x_1/M	x_2/M	P_t/M	P_r/M	m_1^p/M	m_2^p/M	S_1/M^2	S_2/M^2	m_1/M	m_2/M	M_{ADM}/M
RIT	-6.7308	5.5192	0.083116	-0.000490	0.40207	0.51363	-0.08932	0.09963	0.45055	0.54945	0.99141
SXS	-7.8597	6.4004	-	-	-	-	-0.08918	0.09975	0.45020	0.54980	0.99235

- Comparison of the (L, m) = (2, 2) mode extracted from two simulations from SpEC and LazEv.

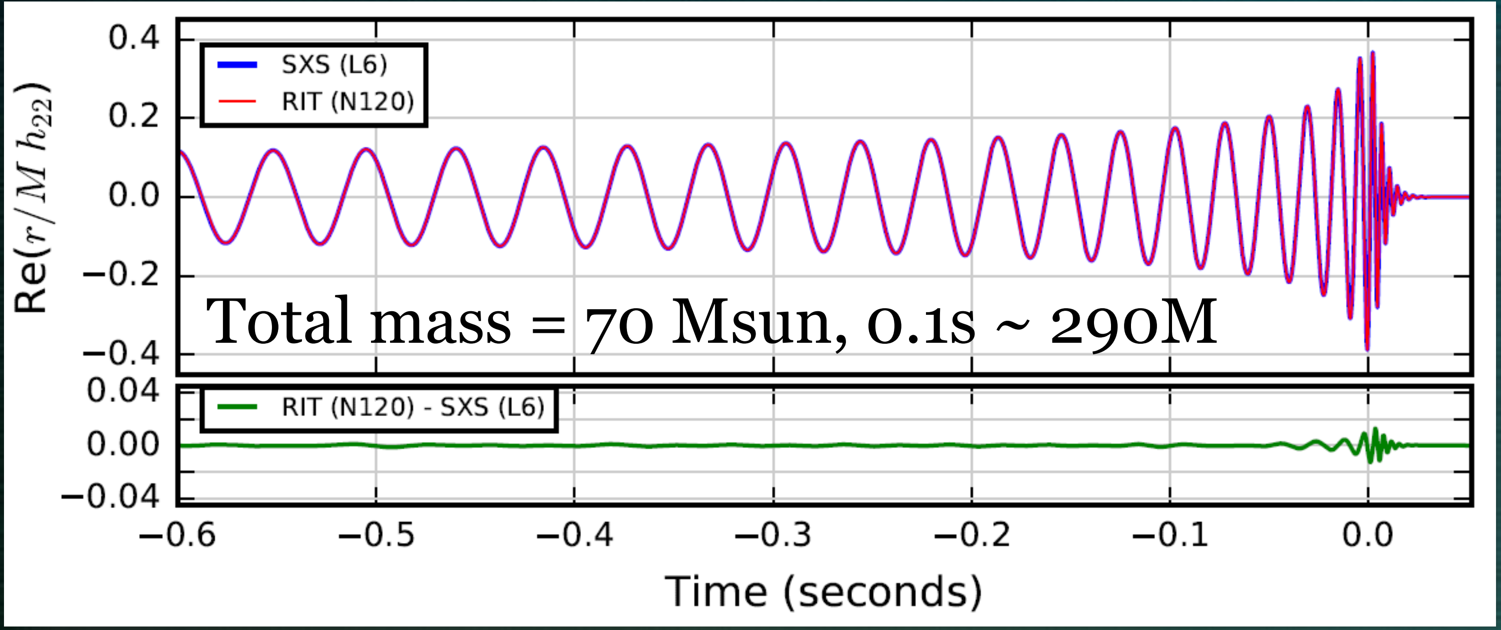

Difference between waveforms

- Quantitative treatment
  - Match (with time and phase shifts only)

$$\mathscr{M} \equiv \frac{\langle h_1 \mid h_2 \rangle}{\sqrt{\langle h_1 \mid h_1 \rangle \langle h_2 \mid h_2 \rangle}},$$

  - Overlap with Advanced LIGO design power spectrum (S_n)

$$\langle h_1 \mid h_2 \rangle = 2 \int_{-\infty}^{\infty} \frac{df}{S_n(f)} \left[\tilde{h}_1(f) \tilde{h}_2(f)^* \right],$$

  - Integration for $|f| \geq f_{min}$

Difference between waveforms

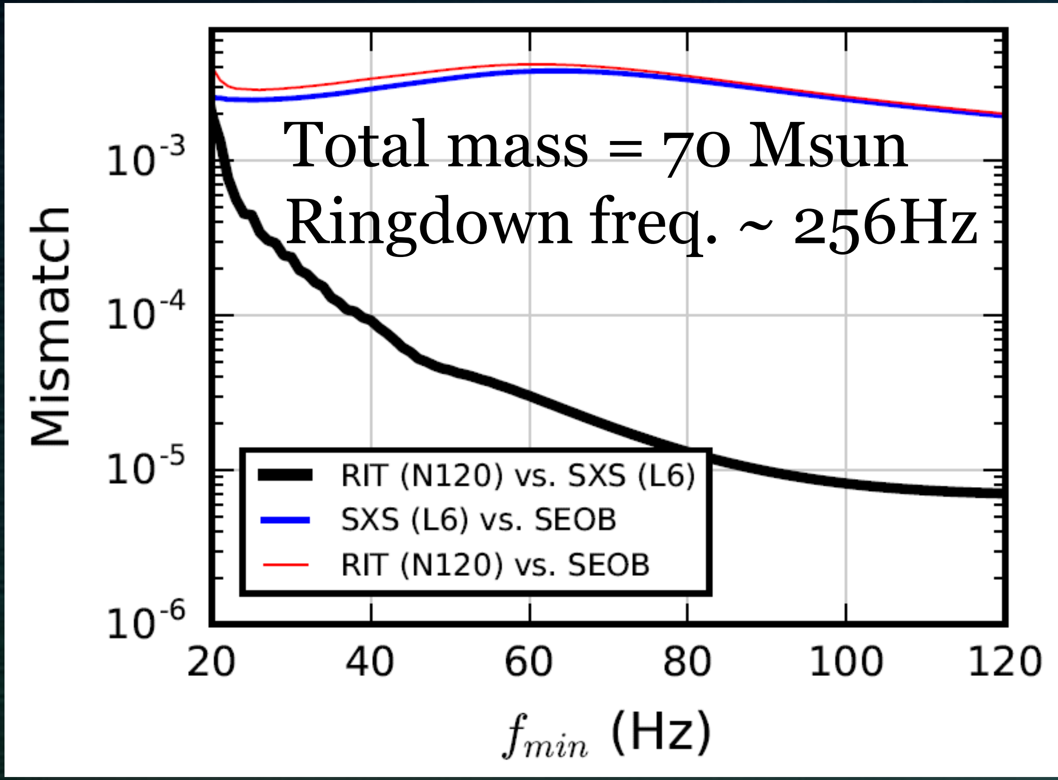

Mismatch **(1-Match)** between SXS (>15.7Hz) and RIT (>19.5Hz) (***L*=2, *m*=2**)-mode waveforms, against one another and against a corresponding SEOBNRv2 (analytical-modeling) template

Difference between waveforms

$f_{min} = 22$ Hz or $22m$ Hz

ℓ	m	$N100$	$N110$	$N120$	$\langle h_{\ell m}^{L6} \| h_{\ell m}^{L6} \rangle$
2	0	0.8854	0.8863	0.8870	9.82
2	1	0.9905	0.9914	0.9908	16.78
2	2	0.9980	0.9980	0.9980	927.74
3	0	0.7822	0.8146	0.8356	1.02
3	1	0.9517	0.9569	0.9582	1.52
3	2	0.9978	0.9980	0.9981	28.59
3	3	0.9927	0.9933	0.9933	42.17
4	0	0.3603	0.3581	0.3554	0.05
4	1	0.7910	0.8348	0.8616	0.17
4	2	0.9074	0.9425	0.9562	1.79
4	3	0.9844	0.9909	0.9938	2.50
4	4	0.9863	0.9886	0.9901	40.95
5	0	0.3638	0.4050	0.4458	0.01
5	1	0.2994	0.3652	0.4227	0.01
5	2	0.6108	0.6176	0.6392	0.14
5	3	0.7813	0.8709	0.9197	0.32
5	4	0.9705	0.9815	0.9879	2.49
5	5	0.9315	0.9552	0.9696	4.94

Match between SXS (L6) and RIT waveforms.

Difference between waveforms

ℓ	m	$N100$	$N110$	$N120$	$\langle h^{L6}_{\ell m} \mid h^{L6}_{\ell m} \rangle$
2	0	0.8854	0.8863	0.8870	9.82
2	1	0.9905	0.9914	0.9908	16.78
2	2	0.9980	0.9980	0.9980	927.74
3	0	0.7822	0.8146	0.8356	1.02
3	1	0.9517	0.9569	0.9582	1.52
3	2	0.9978	0.9980	0.9981	28.59
3	3	0.9927	0.9933	0.9933	42.17
4	0	0.3603	0.3581	0.3554	0.05
4	1	0.7910	0.8348	0.8616	0.17
4	2	0.9074	0.9425	0.9562	1.79
4	3	0.9844	0.9909	0.9938	2.50
4	4	0.9863	0.9886	0.9901	40.95
5	0	0.3638	0.4050	0.4458	0.01
5	1	0.2994	0.3652	0.4227	0.01
5	2	0.6108	0.6176	0.6392	0.14
5	3	0.7813	0.8709	0.9197	0.32
5	4	0.9705	0.9815	0.9879	2.49
5	5	0.9315	0.9552	0.9696	4.94

Dominant (L, m) modes

Difference between waveforms

ℓ	m	$N100$	$N110$	$N120$	$\langle h_{\ell m}^{L6} \vert h_{\ell m}^{L6} \rangle$
2	0	0.8854	0.8863	0.8870	9.82
2	1	0.9905	0.9914	0.9908	16.78
2	2	0.9980	0.9980	0.9980	927.74
3	0	0.7822	0.8146	0.8356	1.02
3	1	0.9517	0.9569	0.9582	1.52
3	2	0.9978	0.9980	0.9981	28.59
3	3	0.9927	0.9933	0.9933	42.17
4	0	0.3603	0.3581	0.3554	0.05
4	1	0.7910	0.8348	0.8616	0.17
4	2	0.9074	0.9425	0.9562	1.79
4	3	0.9844	0.9909	0.9938	2.50
4	4	0.9863 -->	0.9886 -->	0.9901	40.95
5	0	0.3638	0.4050	0.4458	0.01
5	1	0.2994	0.3652	0.4227	0.01
5	2	0.6108	0.6176	0.6392	0.14
5	3	0.7813	0.8709	0.9197	0.32
5	4	0.9705	0.9815	0.9879	2.49
5	5	0.9315 -->	0.9552 -->	0.9696	4.94

-----> Higher resolution

Difference between waveforms

ℓ	m	$N100$	$N110$	$N120$	$\langle h^{L6}_{\ell m} \| h^{L6}_{\ell m} \rangle$
2	0	0.8854	0.8863	0.8870	9.82
2	1	0.9905	0.9914	0.9908	16.78
2	2	0.9980	0.9980	0.9980	927.74
3	0	0.7822	0.8146	0.8356	1.02
3	1	0.9517	0.9569	0.9582	1.52
3	2	0.9978	0.9980	0.9981	28.59
3	3	0.9927	0.9933	0.9933	42.17
4	0	0.3603	0.3581	0.3554	0.05
4	1	0.7910	0.8348	0.8616	0.17
4	2	0.9074	0.9425	0.9562	1.79
4	3	0.9844	0.9909	0.9938	2.50
4	4	0.9863	0.9886	0.9901	40.95
5	0	0.3638	0.4050	0.4458	0.01
5	1	0.2994	0.3652	0.4227	0.01
5	2	0.6108	0.6176	0.6392	0.14
5	3	0.7813	0.8709	0.9197	0.32
5	4	0.9705	0.9815	0.9879	2.49
5	5	0.9315	0.9552	0.9696	4.94

Worse for lower m modes

Extrapolating gravitational-wave data

- Taylor series fitting with respect to $\frac{1}{r}$ in SXS

$$A = \sum \frac{A_{(n)}}{r^n}$$

Boyle and Mroué, Phys. Rev. D 80, 124045 (2009).

- Perturbative extrapolation

$$r\psi_4^{\ell m}|_{r=\infty} = \left(1 - \frac{2M}{r}\right)\left(r\psi_{4\ell m}^{\mathrm{NR}}(t,r) - \frac{(\ell-1)(\ell+2)}{2r}\int dt[r\psi_{4\ell m}^{\mathrm{NR}}(t,r)]\right.$$
$$\left. + \frac{(\ell-1)(\ell+2)(\ell^2+\ell-4)}{8r^2}\int\int dt dt[r\psi_{4\ell m}^{\mathrm{NR}}(t,r)]\right)$$

$$\int dt \rightarrow \frac{1}{\omega}, \qquad \omega = m\sqrt{M/r_0^3}$$

Brief summary

- The length of the waveforms for lower masses is challenging to model with pure NR.
- It is more efficient to match the early part of the binary evolution to PN waveforms and build up a hybrid data-bank.

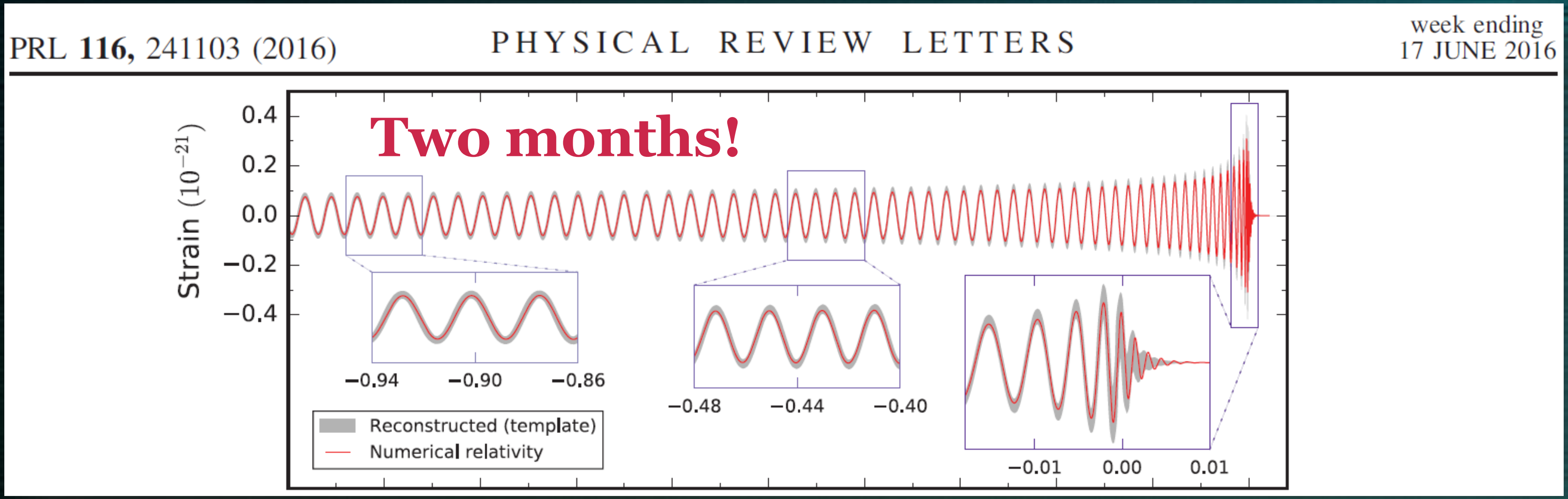

--- By Carlos O. Lousto in GR21

Brief summary

- The length of the waveforms for lower masses is challenging to model with pure NR.
- It is more efficient to match the early part of the binary evolution to PN waveforms and build up a hybrid data-bank.
- Challenging corners of the parameter space: small mass ratios and high spins.
- Still NR to provide further simulations for BH/NS and NS/NS systems.

--- By Carlos O. Lousto in GR21

Ringdown gravitational waves

- Did we really observe the ringdown waves?

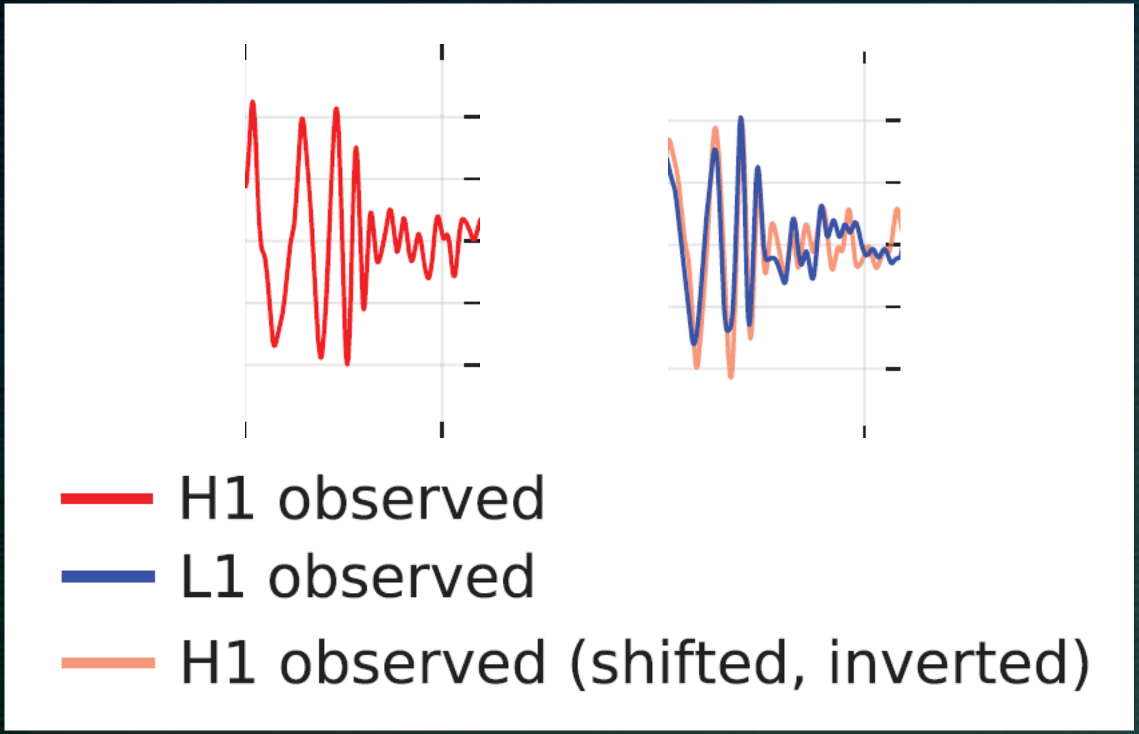

LIGO Scientific Collaboration
and Virgo Collaboration,
Phys. Rev. Lett. 116, 061102 (2016).

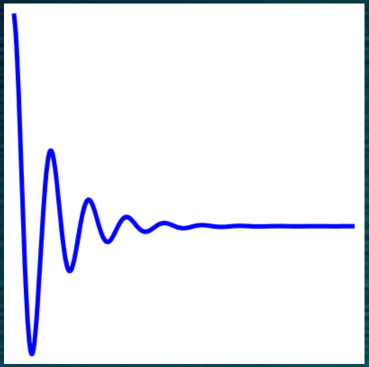

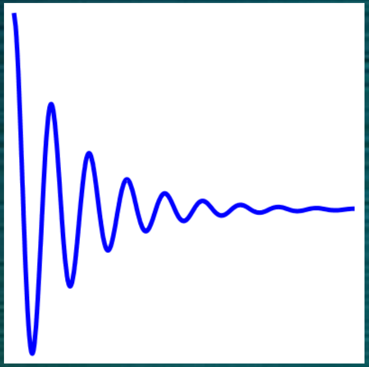

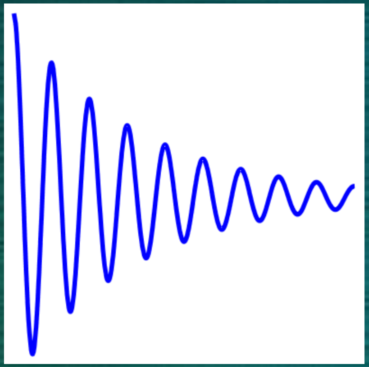

Ringdown gravitational waves

- Did we really observe the ringdown waves?

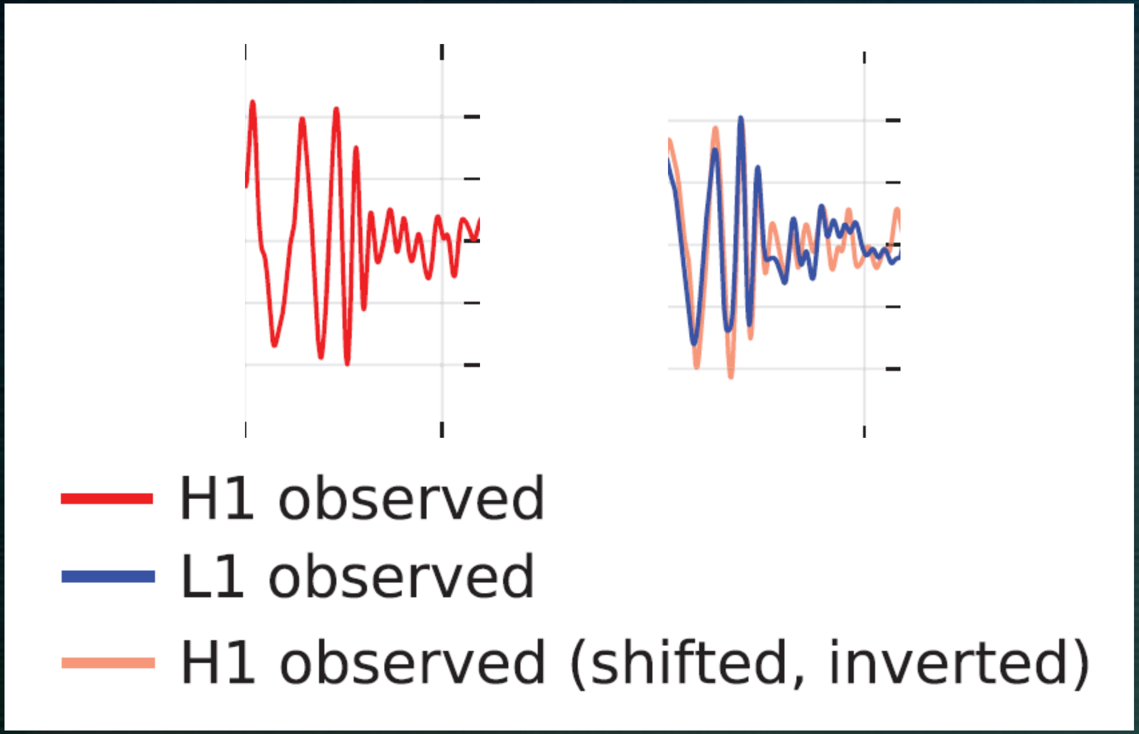

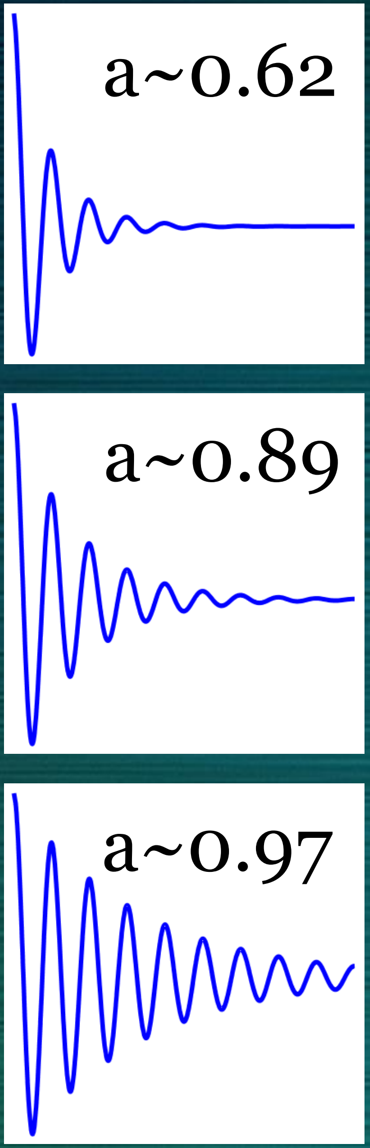

LIGO Scientific Collaboration
and Virgo Collaboration,
Phys. Rev. Lett. 116, 061102 (2016).

Ringdown of GW150914

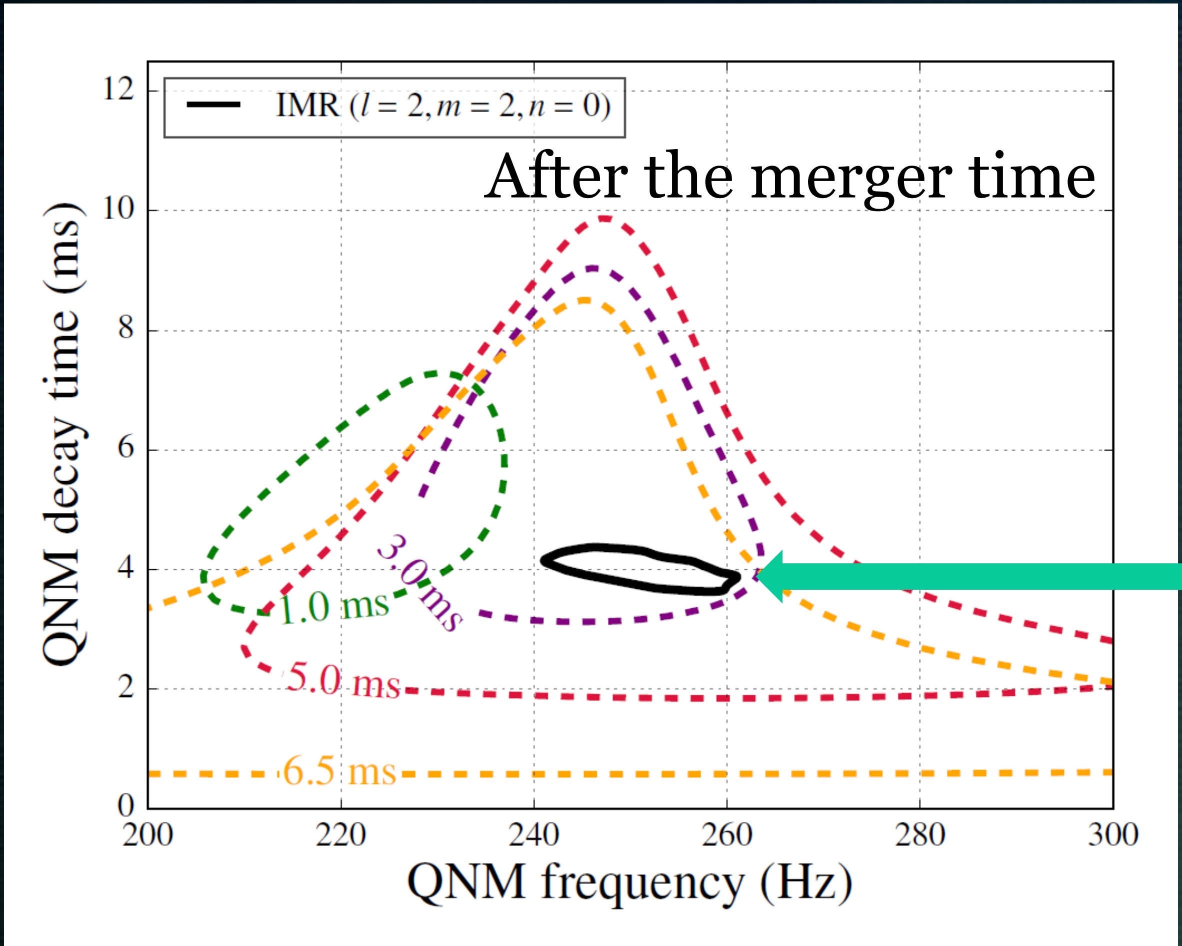

Derived from the full waveform

LIGO Scientific Collaboration and Virgo Collaboration, Phys. Rev. Lett. 116, 221101 (2016).

Ringdown and quasinormal modes

- Ringdown GWs are described by damped sinusoidal waves.

$$h \propto \exp\left[-\pi f_c (t - t_0)/Q\right] \cos(2\pi f_c (t - t_0) - \phi_0)$$

  - Central frequency: f_c, quality factor: Q, t_0, φ_0: initial time and phase

- If the remnant is BH, then BH's QNMs! The dominant (L=2, m=2), least-damped (n=0) mode

$$\begin{aligned} f_c &= \frac{1}{2\pi M_{\rm rem}} \left[1.5251 - 1.1568(1 - \alpha_{\rm rem})^{0.1292}\right] \\ &= 538.4 \left(\frac{M_{\rm rem}}{60 M_\odot}\right)^{-1} \left[1.5251 - 1.1568(1 - \alpha_{\rm rem})^{0.1292}\right] \, [\mathrm{Hz}] \, , \\ Q &= 0.7000 + 1.4187(1 - \alpha_{\rm rem})^{-0.4990} \, , \end{aligned}$$

Berti, Cardoso and Will, Phys. Rev. D 73, 064030 (2006).

Simple GR test

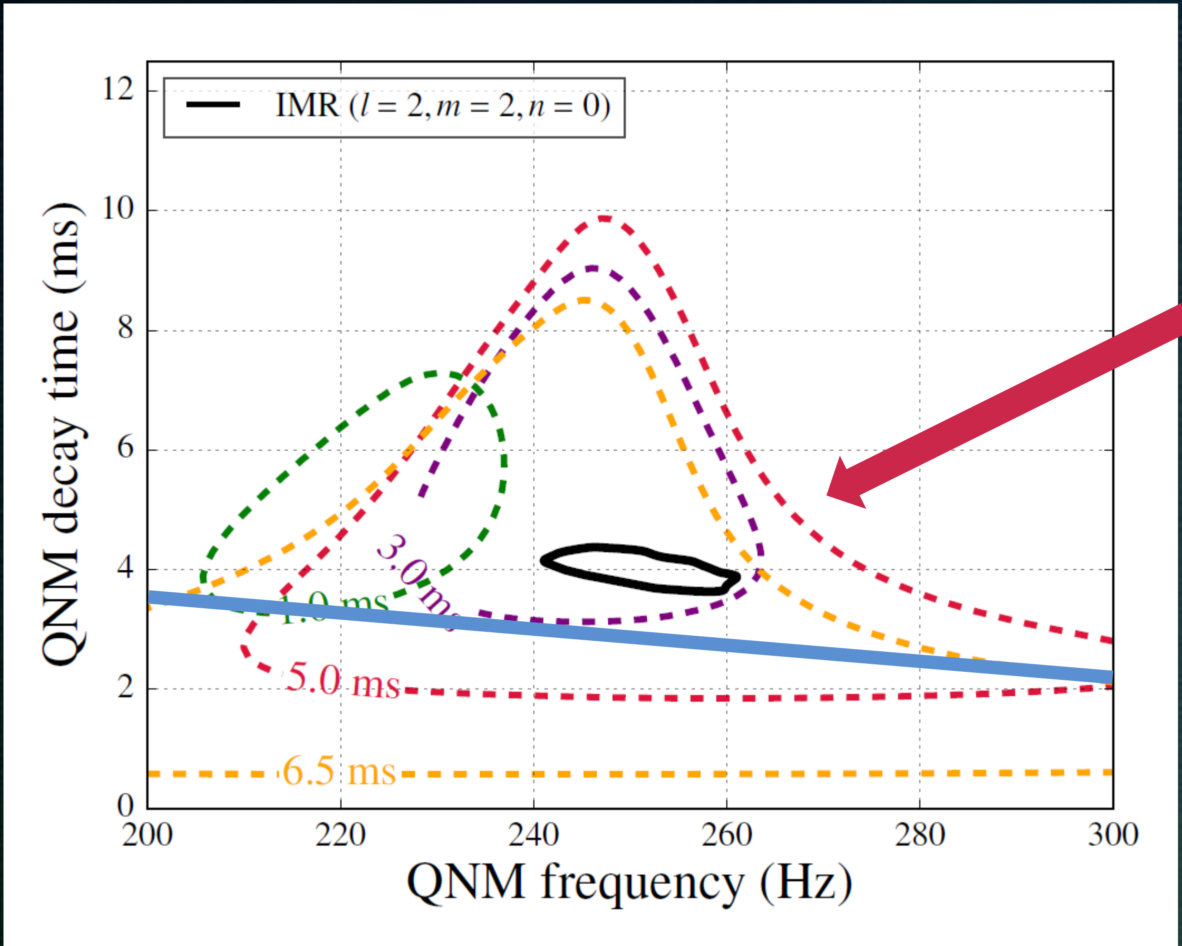

(5.0ms)
SNR ~ 6.3, 90% CL

Schwarzschild line ($\alpha_{rem} = 0$):
If below the line, something wrong in GR.

Ringdown (real and imaginary freq.)

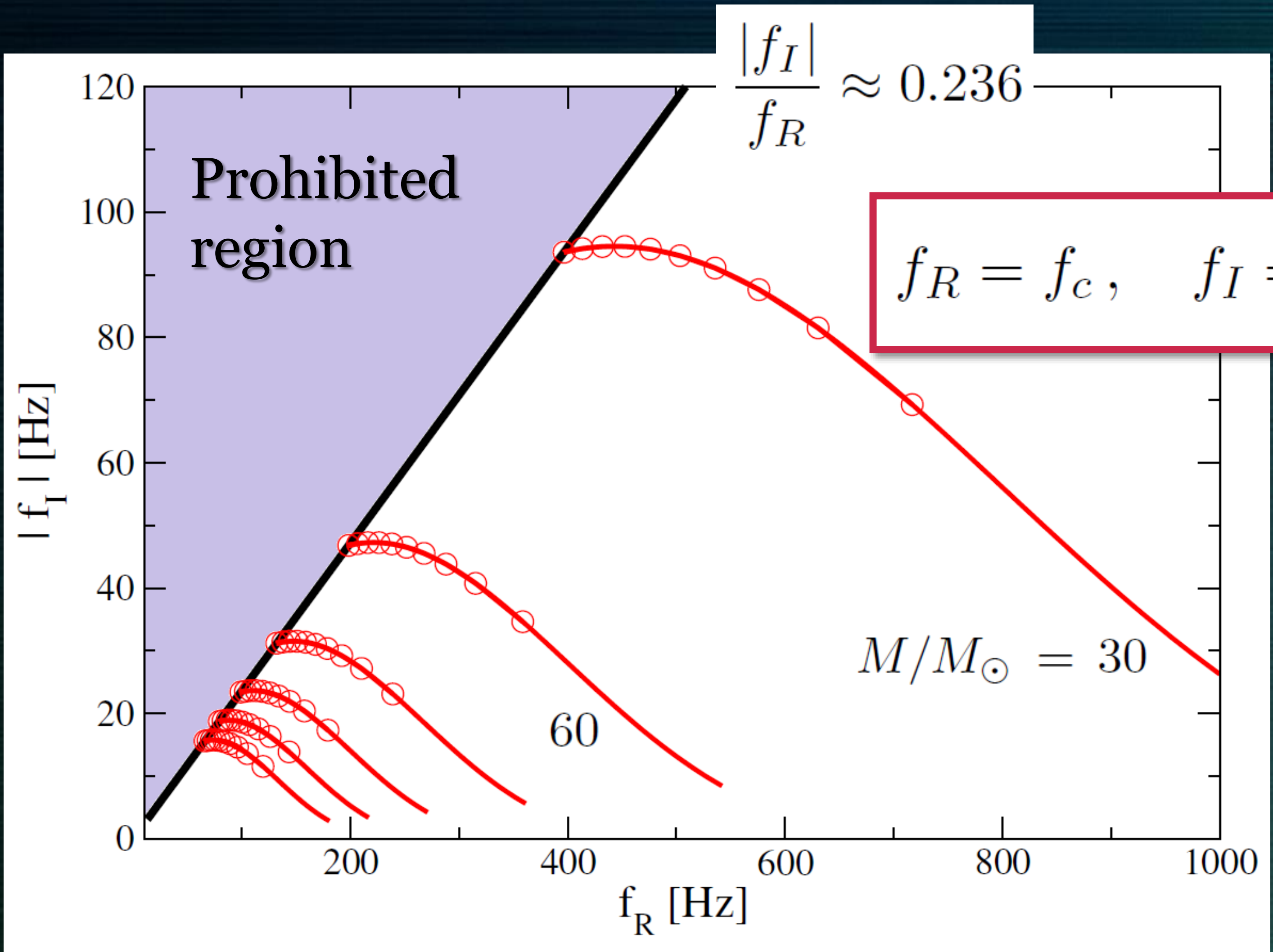

$$f_R = f_c\,, \quad f_I = -\frac{f_c}{2Q}$$

Nakano, Tanaka, Nakamura, Phys. Rev. D92, 064003 (2015).

Typical Pop III BBHs

(Kinugawa-san)

Kinugawa, Inayoshi, Hotokezaka, Nakauchi and Nakamura, MNRAS 442, 2963 (2014).

Kinugawa, Miyamoto, Kanda and Nakamura, MNRAS 456, 1093 (2016).

- **Total mass: 60M_sun, equal mass**
- (assuming nonspinning BBHs)
- Simply use the phenomenological fitting formulas for the remnant mass and spin

Healy, Lousto and Zlochower, Phys. Rev. D 90, 104004 (2014).

Simple GR test

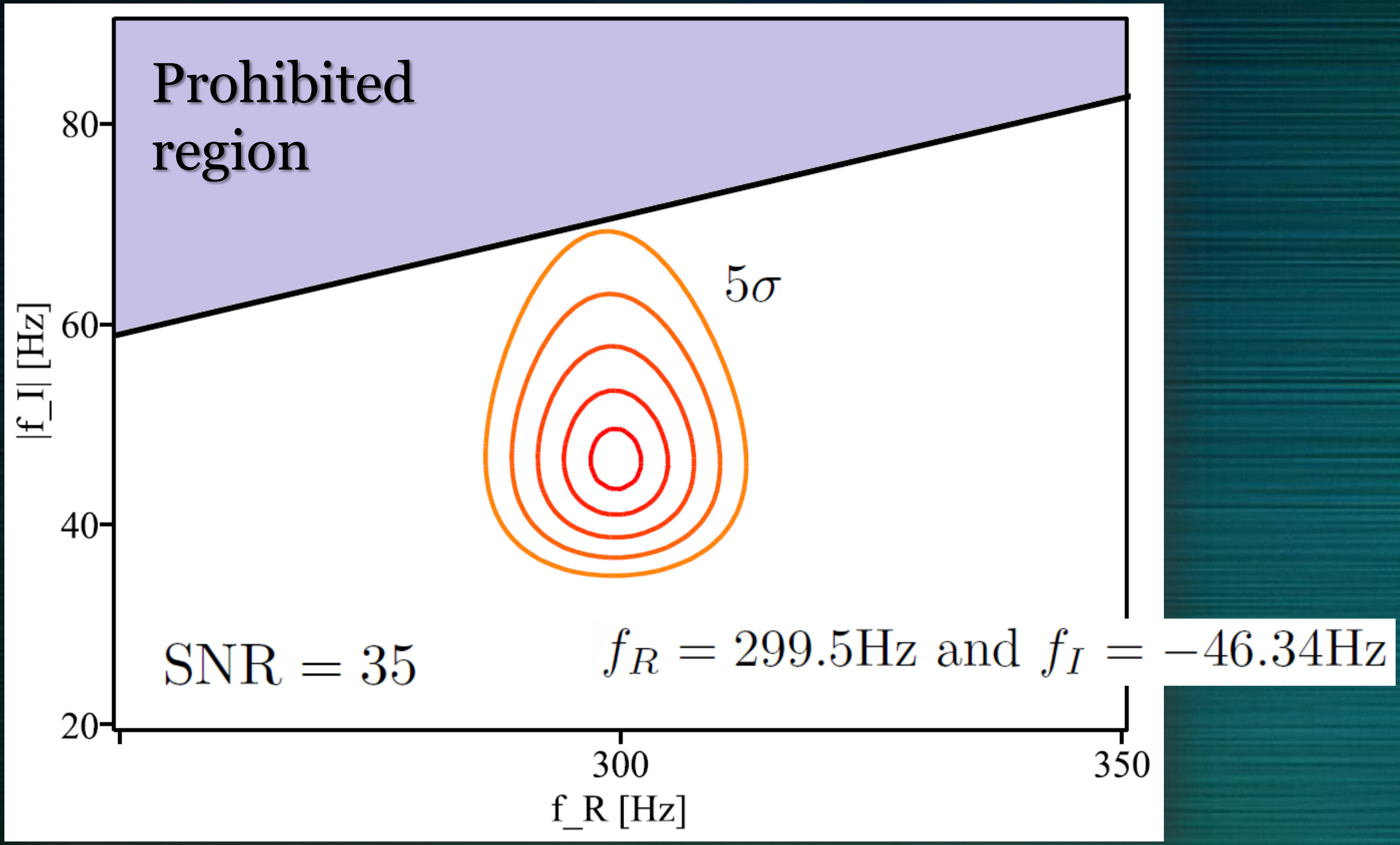

Kinugawa, Nakano, Nakamura, arXiv:1606.00362

SNR=35?

Event	$M_{\rm rem}/M_\odot$	$\alpha_{\rm rem}$
GW150914	62.3	0.68
LVT151012	35	0.66
GW151226	20.8	0.74

LIGO Scientific Collaboration and Virgo Collaboration, arXiv:1606.04856

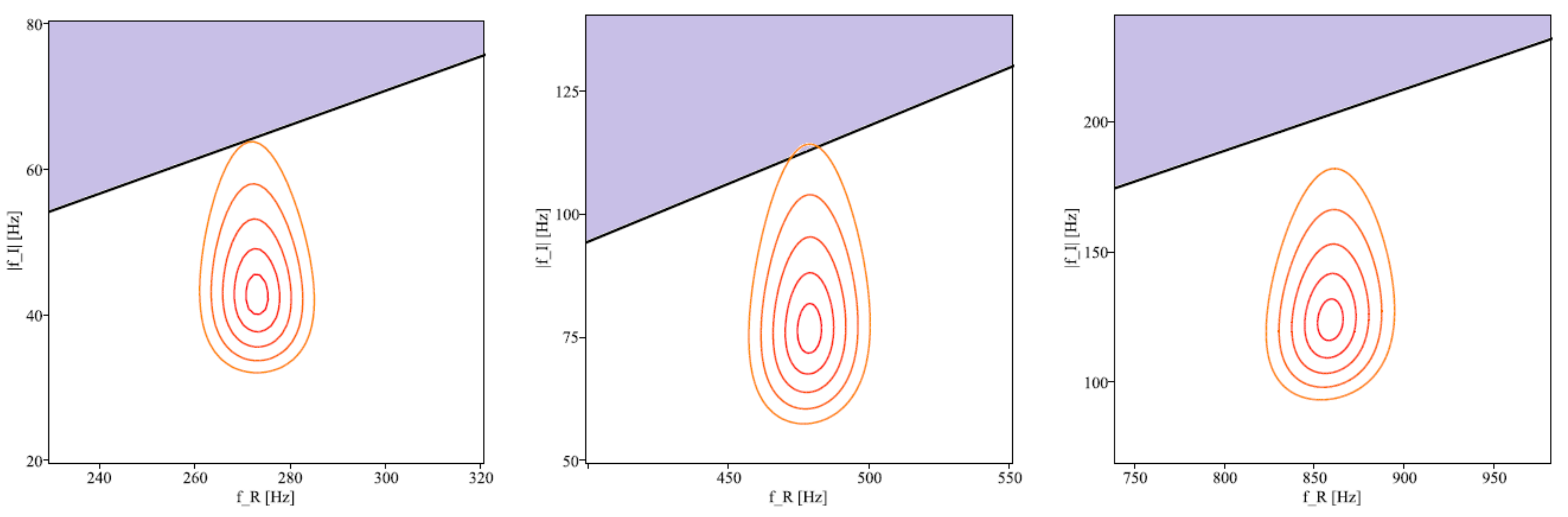

GW150914 LVT151012 GW151226

With B-DECIGO

(Sato-san)

SNR for ringdown GW

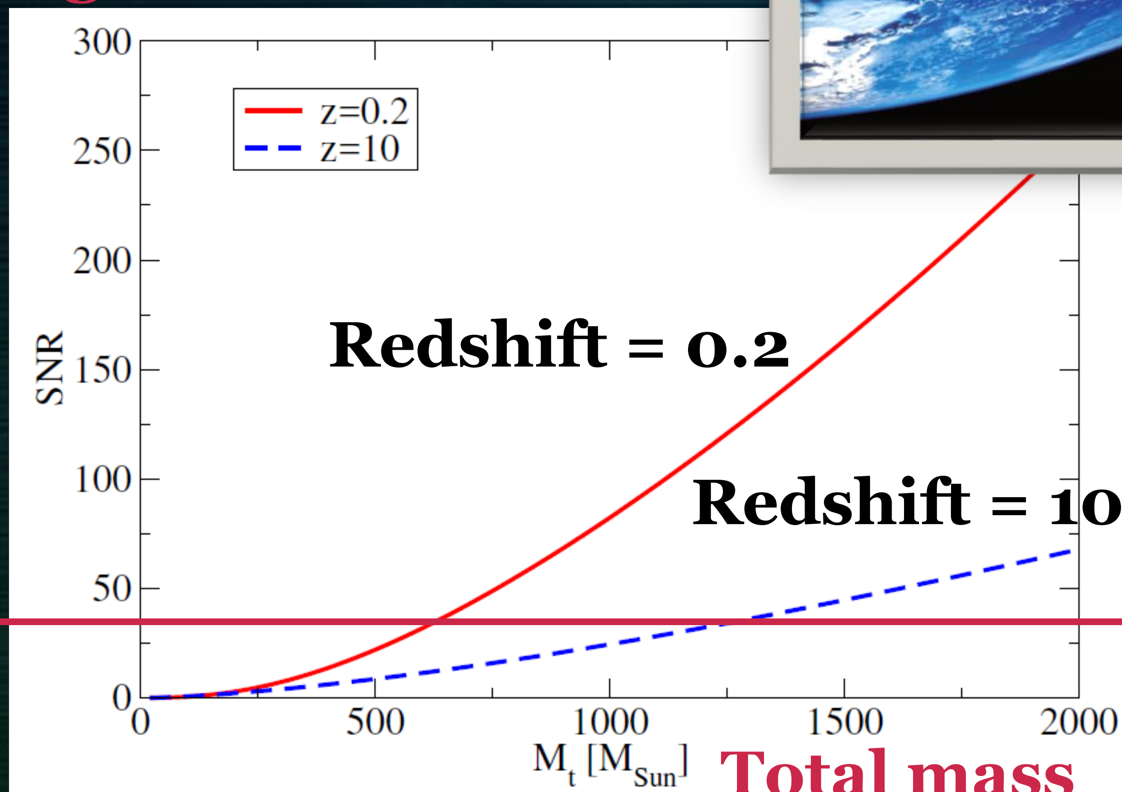

SNR=35

Total mass

T. Nakamura et al., Prog. Theor. Exp. Phys. 093E01 (2016) [arXiv:1607.00897 [astro-ph.HE]].

Summary

- Strong test by numerical relativity
- Simple GR test with QNM
  - Cf. Testing GR (BH) with multi QNMs
- Main stream (?) Extraction of Ringdown GWs is important!

Inspiral phase $(m_1, m_2, \boldsymbol{S}_1, \boldsymbol{S}_2)$	**Merger phase** Numerical relativity --> Fitting formula	Ringdown phase $(M_{\mathrm{rem}}, \alpha_{\mathrm{rem}})$ QNM spectrum

- **New physics** from deviation
- Yagi-san's presentation on "Probing Various Gravitational Theories"

Kerr BH and QNMs

- Starting from Kerr metric

$$
\begin{aligned}
ds^2 &= -\left(1-\frac{2Mr}{\Sigma}\right)dt^2 - \frac{4Mar\,\sin^2\theta}{\Sigma}dtd\phi + \frac{\Sigma}{\Delta}dr^2 + \Sigma d\theta^2 \\
&\quad + \left(r^2+a^2+\frac{2Ma^2r}{\Sigma}\sin^2\theta\right)\sin^2\theta d\phi^2\,,
\end{aligned}
$$

$\Sigma = r^2 + a^2\cos^2\theta$ $\quad$ $\Delta = r^2 - 2Mr + a^2$

- Master equation for perturbations

Teukolsky equation

$$\Delta^2 \frac{d}{dr}\frac{1}{\Delta}\frac{dR}{dr} - VR = -T\,,$$

S. A. Teukolsky, ApJ. 185, 635 (1973).

Sasaki-Nakamura equaiton

- V: Potential of radial Teukolsky Eq.: Long-range

$$\Delta^2 \frac{d}{dr}\frac{1}{\Delta}\frac{dR}{dr} - VR = 0 \;,$$

For QNMs, vacuum perturbation

- To short-range one
  Sasaki, Nakamura, Phys. Lett. A **89**, 68 (1982).
  Sasaki, Nakamura, Prog. Theor. Phys. **67**, 1788 (1982).
  Nakamura, Sasaki, Phys. Lett. A **89**, 185 (1982).

$$\frac{d^2Y}{dr^{*2}} + \left(\omega^2 - V_{\rm SN}\right) Y = 0 \,,$$

$$\frac{dr^*}{dr} = \frac{r^2+a^2}{\Delta} \,.$$

WKB analysis of QNMs

- Schutz and Will, ApJ, 291, L33 (1985).

QNM GWs from potential peak

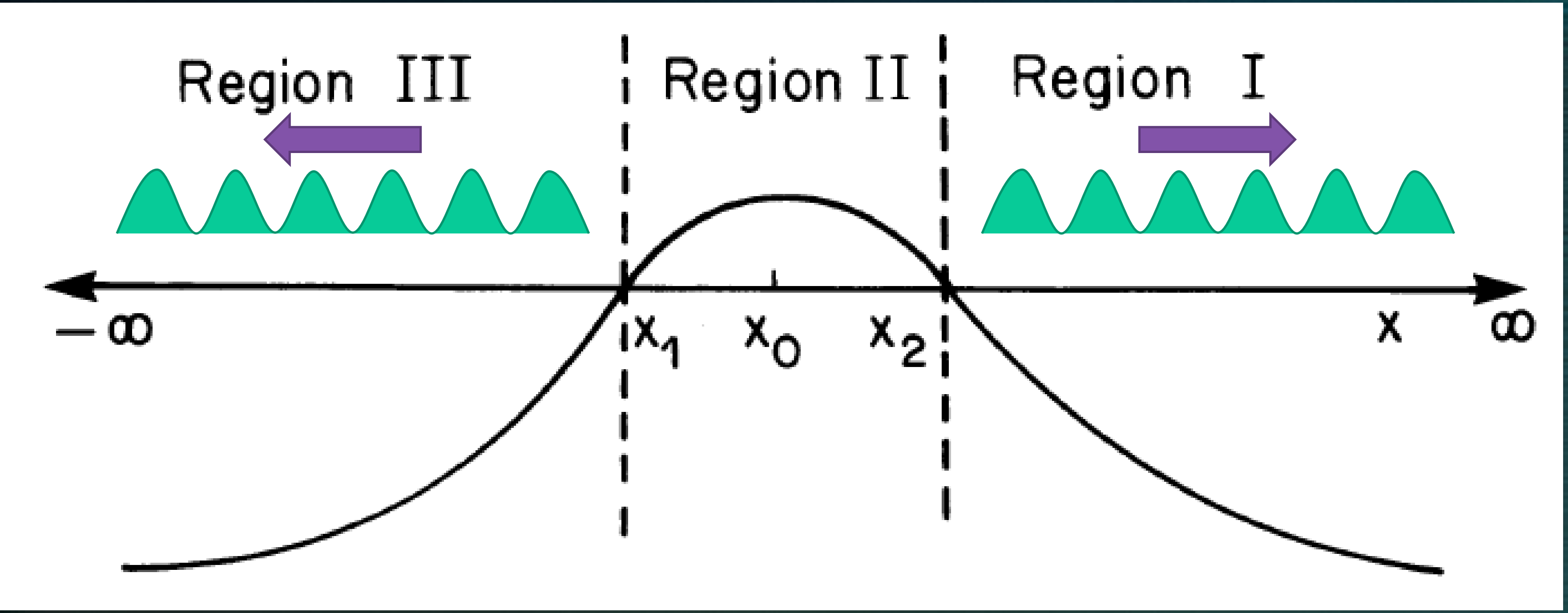

QNM Freq. --> Location of GW emission

- Nakamura, Nakano, Tanaka, Phys. Rev. D 93, 044048 (2016).

Accuracy in WKB

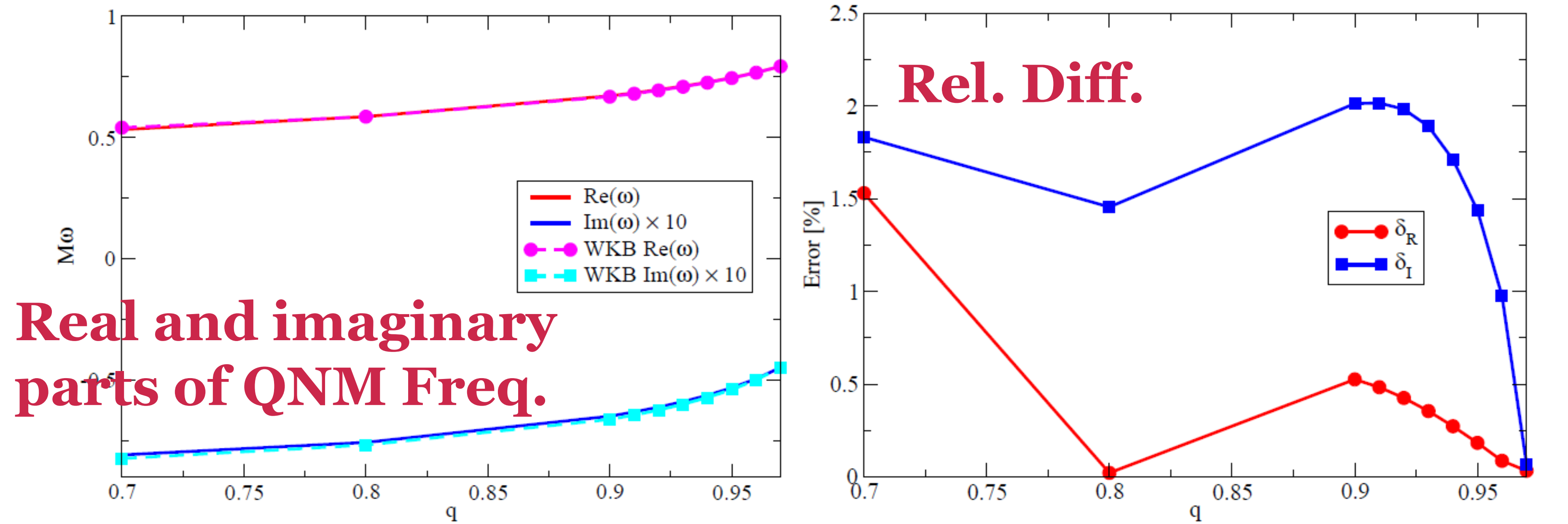

Nondimensional spin parameter

Fig. 4 (Left) The real and imaginary parts of the fundamental ($n = 0$) QNM frequencies with $V_D(\ell = 2, m = 2)$ evaluated for various spin parameters $q = a/M$. The exact frequencies $\mathrm{Re}(\omega)$ and $\mathrm{Im}(\omega)$ are from Ref. [26, 27]. (Right) Absolute value of relative errors for the real and imaginary part of the QNM frequencies with $V_D(\ell = 2, m = 2)$, $\delta_R = |(\mathrm{WKB}\ \mathrm{Re}(\omega))/\mathrm{Re}(\omega) - 1|$ and $\delta_I = |(\mathrm{WKB}\ \mathrm{Im}(\omega))/\mathrm{Im}(\omega) - 1|$ between the exact value and that of the WKB approximation.

Uncertainty of peak location

- An analysis for the uncertainty
(in the limit of spin parameter, q=a/M → 1)
Nakano, Sago, Tanaka, Nakamura,
Prog. Theor. Exp. Phys., 083E01 (2016).

- Peak location:

$$\frac{r_{\rm p}}{M} \lesssim 1 + 1.8\,(1-q)^{1/2}\,.$$

- Event horizon:

$$\begin{aligned} r_+/M &= 1+\sqrt{1-q^2} \\ &= 1+\sqrt{2}\,(1-q)^{1/2}+O((1-q)^{3/2})\,, \end{aligned}$$

Various radius

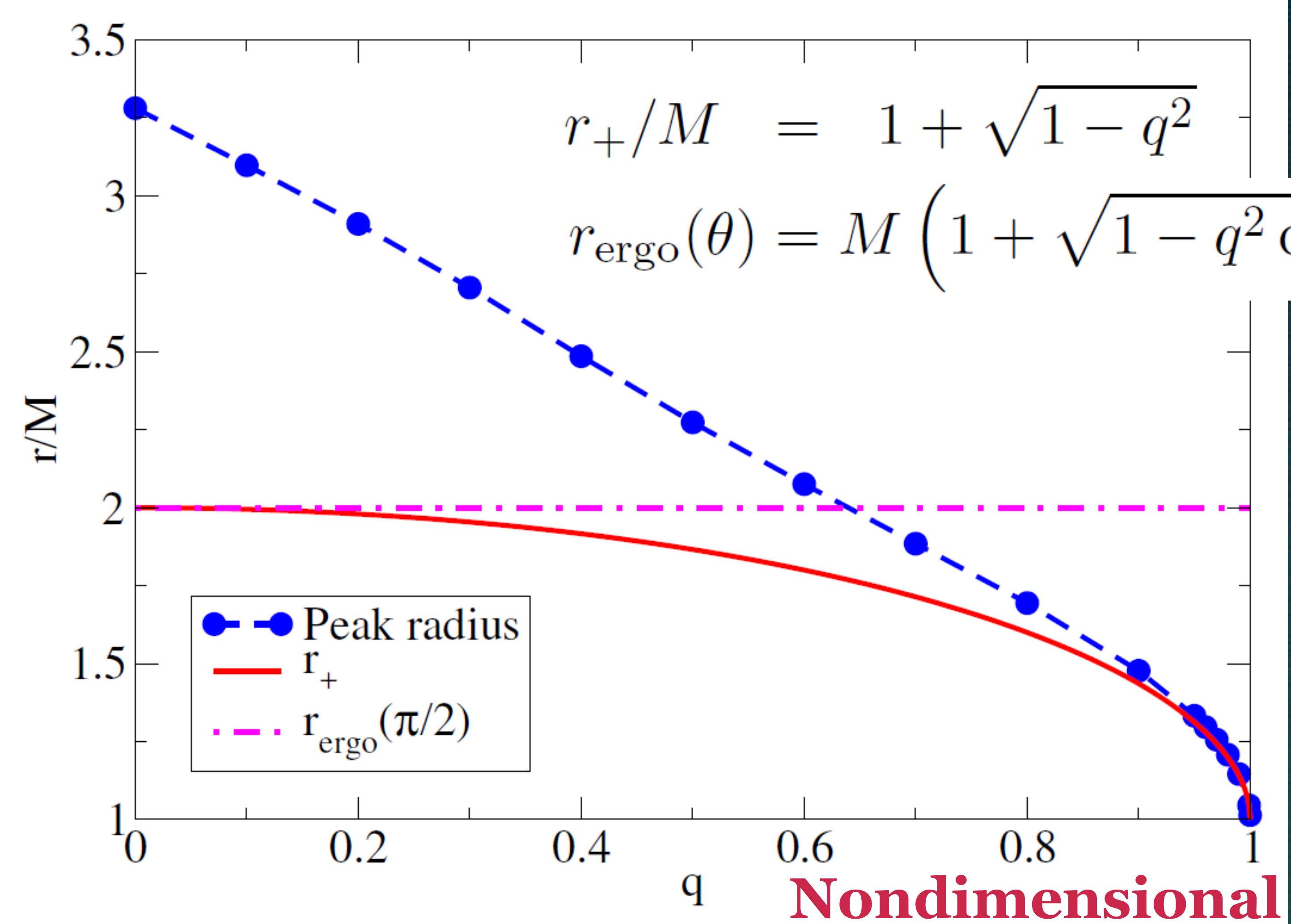

$$r_+/M = 1 + \sqrt{1 - q^2}$$

$$r_{\rm ergo}(\theta) = M\left(1 + \sqrt{1 - q^2 \cos^2\theta}\right)$$

Nondimensional spin

Nakamura, Nakano,
Prog. Theor. Exp. Phys., 041E01 (2016).